Vol. 683: 109–121, 2022
https://doi.org/10.3354/meps13931

MARINE ECOLOGY PROGRESS SERIES
Mar Ecol Prog Ser

Published February 3

Effects of environmental factors within the spawning area and migration routes on the length of *Anguilla japonica* glass eels recruited to Taiwan

Kuan-Mei Hsiung[1,2,#], Chi Ma[2,#], Chia-Ying Ko[2,3,4,#], Yu-Heng Tseng[5], Yi-Chun Kuo[5], Yu-San Han[2,3,*]

[1]School of Oceanography, Shanghai Jiao Tong University, No.1954 Huashan Road, Shanghai 200030, PR China
[2]Institute of Fisheries Science, College of Life Science, National Taiwan University, No.1 Roosevelt Road, Daan District, Taipei City 10617, Taiwan
[3]Department of Life Science, College of Life Science, National Taiwan University, No.1 Roosevelt Road, Daan District, Taipei City 10617, Taiwan
[4]Department of Biochemical Science and Technology, College of Life Science, National Taiwan University, No.1 Roosevelt Road, Daan District, Taipei City 10617, Taiwan
[5]Institute of Oceanography, College of Science, National Taiwan University, No.1 Roosevelt Road, Daan District, Taipei City 10617, Taiwan

ABSTRACT: Growth extent varies considerably among recruiting cohorts of Japanese eels *Anguilla japonica*. However, the effects of oceanic variation on their growth, particularly during the larval stage, remain unclear. We sampled glass eels in northeast Taiwan from 2010 to 2019 and investigated the effects of sea surface temperature (SST), salinity, chlorophyll *a* (chl *a*) concentration, and El Niño–Southern Oscillation (ENSO) events on the total length (TL) of these eels by developing a generalized additive model. The results revealed that mean SST between 21 and 24.5°C in the spawning area was associated with TL. Larger TL values were observed from 0.03–0.07 mg m^{-3} in the spawning area, and along the migration routes TL was greatest when chl a was > 13 mg m^{-3}. Other variables, including mean SST and salinity along the migration route, influenced TL but contributed less than 4.5%. Larger and smaller *A. japonica* glass eels were observed during El Niño and La Niña years, respectively. Specifically, El Niño years exerted the greatest influence (67.1%) on TL, and this was followed by mean SST (12%) and accumulated chl *a* concentration (11.4%) within the spawning area. Our results indicated that environmental factors within the spawning area influenced the TL of *A. japonica* glass eels to a greater extent than did those along the migration routes, and climatic ENSO events exerted an additional important effect regarding changes in TL. Taken together, our results provide fundamental ecological information and a basis for fisheries to more effectively manage *A. japonica*.

KEY WORDS: *Anguilla japonica* · Leptocephali metamorphosis · Larval transport processes · Recruitment dynamics · Environmental changes

1. INTRODUCTION

The Japanese eel *Anguilla japonica* is a catadromous fish with a complicated life history. Its spawning area is located at approximately 142–143° E in the North Equatorial Current (NEC) to the west of the Mariana Ridge (Tsukamoto 1992, 2006, 2009, Tsukamoto et al. 2011) (see Fig. 1). Mature *A. japonica* individuals spawn from May to August, and after hatching, the larvae (leptocephali) drift passively from the spawning area for the next 4–6 mo before metamorphosing into juvenile eels (glass eels) and reach-

[#]Co-first authors
[*]Corresponding author: yshan@ntu.edu.tw

ing the East Asian coasts (Tsukamoto 1992, 2006, Cheng & Tzeng 1996, Han et al. 2012). The NEC bifurcates at its westernmost boundary near the coast of the Philippines into the north-flowing Kuroshio and south-flowing Mindanao Current (MC); this feature is known as the NEC bifurcation (Nitani 1972, Toole et al. 1990). *A. japonica* larvae must enter the Kuroshio within the bifurcation zone to reach their habitats in East Asian countries (Tabeta & Takai 1975, Shinoda et al. 2011). The maximum mean (±SD) zonal velocity of the NEC reaches 30± 12 cm s^{-1} (Zhang et al. 2017), which is faster than the swimming ability of *A. japonica* larvae after hatching (3.6 ± 2.7 cm s^{-1} based on a tank experiment) (Yamada et al. 2009). Additionally, as the larvae drift with the current, they remain in the upper surface waters at night (approximately 50 m deep) and evade predators in the daytime by diving into deeper waters (approximately 150 m deep) (Kajihara 1988, Otake et al. 1998). This behavior is known as diel vertical migration (DVM). Given that the early life stages of *A. japonica* within the oceans are the most vulnerable periods during their growth and development, improved knowledge of how biological and physical changes in oceanic environmental conditions can influence larval transport processes, mortality, and growth rates is critical to understanding the recruitment dynamics of the species and for developing appropriate fisheries management strategies (Kimura et al. 1994, Houde 2008, Chang et al. 2015).

A. japonica is one of the most important eel species in the fisheries and aquaculture industries in East Asia. As artificial reproduction of the eels has not been successful on a commercial scale (Tanaka 2003), the supply of eel fry for aquaculture is highly dependent upon the juvenile eels harvested in estuarine/coastal waters during their recruitment period (Cheng & Tzeng 1996, Liao 2001, Tzeng 2003). However, populations of *A. japonica* began to decline in the 1970s (Dekker 2004), earlier than declines in other eel species occurred, and the species is currently listed as Endangered on the IUCN Red List (Jacoby & Gollock 2014). After approximately 2010, annual recruitment declined by as much as 90% compared to the eel catch in the 1960s (Jacoby & Gollock 2014). Consequently, the fishery resources specific for *A. japonica* face a major challenge.

Numerous studies have focused on climate change and habitat loss as potential reasons for eel population declines, and these studies have yielded a large body of research involving eel fisheries resource management. For example, researchers have explored the impacts of oceanic–atmospheric changes on the transport processes and recruitment dynamics of *A. japonica*, and these studies have examined the influences of the El Niño–Southern Oscillation (ENSO) events, the Philippines–Taiwan Oscillation, and global warming on the annual catch and catch per unit effort (CPUE) in Japan and have also investigated the larval duration in oceanic current systems, the recruitment index of the arrival of *A. japonica* in estuaries in proximity to Taiwan, and the larval distribution after entering the Kuroshio (Kimura et al. 2001, Kim et al. 2007, Zenimoto et al. 2009, Chang et al. 2015, Han et al. 2016, Hsu et al. 2017, Hsiung et al. 2018, Han et al. 2019, Hsiung & Kimura 2019). However, few studies have examined the relative roles of environmental factors that influence eel larval biological processes. Investigations examining how different temporal and environmental conditions affect larval growth, transport, and dispersal should offer insights that will serve to facilitate eel resource management and conservation.

Previous studies have reported that physiological and metabolic activity, behavior, and growth in the early life stages of fish are temperature-sensitive (Blaxter 1991), and this is particularly true in regards to growth (Houde 2008). Additionally, high survival and growth rates of fish larvae are typically associated with high prey levels (Rilling & Houde 1999, Zenitani et al. 2007), as low prey levels may limit larval growth and lead to poor nutritional conditions in the marine environment, ultimately increasing larval susceptibility to predation. The life history of eel larvae involves 2 stages: the leptocephalus stage, in which growth is dependent upon food supply, and the glass eel stage, where feeding and growth are halted until immigration into estuarine waters. Cohorts of fast-growing larvae that achieve large sizes earlier in their development experience lower cumulative stage-specific mortality and exhibit a higher recruitment probability, thus implying that large sizes and rapid growth may enhance survival potential (Houde 1989, Anderson 1998).

In the European eel *Anguilla anguilla*, Gascuel (1986) demonstrated a positive correlation between the upstream migration of glass eels in the estuary and temperature in spring. Elie & Rochard (1994) further suggested that the migration and recruitment of glass eels are both affected by temperature differences that may be caused by the difference between the sea and freshwater areas. These results indicate that temperature influences the migratory behavior of eels. Additionally, Bonhommeau et al. (2008) demonstrated a strong and significant negative relationship between fluctuations in sea temperature

and the glass eel recruitment index. Low sea surface temperature (SST) periods were associated with high glass eel recruitment that could be due to the strong positive correlation observed between the glass eel recruitment index and primary production (PP) in the eel spawning area in addition to the negative correlation between PP and SST in the Sargasso Sea (Bonhommeau et al. 2008). Furthermore, Aoki et al. (2018) revealed that yearly CPUE was extremely high when the lowest SST was observed in the waters adjacent to the Oyodo River Estuary due to enhanced riverine circulation. Additionally, *A. anguilla* glass eels appear to prefer swimming toward less saline waters (Tosi et al. 1990), whereas *A. japonica* mature eels are known to spawn just south of the salinity front (Kimura et al. 1994, Kimura & Tsukamoto 2006, Aoyama et al. 2014, Takeuchi et al. 2021). Therefore, shifts in salinity could be a major cue for eel migration and spawning. In summary, environmental factors such as PP, salinity, and SST may play key roles in eel migration, thus influencing mortality, growth rate, food availability, and the migration process.

This study represents the first attempt to combine long-term body length data (representing the growth of *A. japonica*) and particle tracking (simulating the migration routes) with environmental variables such as SST, salinity, and chlorophyll *a* (chl *a*) concentration as a proxy for phytoplankton biomass and for PP to investigate the effects of environmental changes in the spawning area and migration routes on *A. japonica* larval growth. The underlying basis for this study involves previous observations regarding the ability of inter-annual variability of oceanic currents to affect larval dispersal and the ability of environmental conditions during larval migration to affect larval growth. Both of these factors exert significant effects on eel recruitment dynamics, including arrival time, catch amounts, and fisheries duration, in coastal areas. Therefore, we used the eels that were captured as representatives. In this study, 9 yr (2010–2019) body length data of *A. japonica* glass eels captured in waters northeast of Taiwan were measured, and spawning dates were estimated by combining the glass eel daily age and the date of the new moon (see Section 2.1). Subsequently, a particle transport model was used to simulate the migration routes and to extract fluctuations in accumulated chl *a* concentrations, salinity, and SST that the eel larvae experienced within the spawning locations. Previous studies have demonstrated that migration success and drifting time could be influenced by ENSO events (Kim et al. 2007, Zenimoto et al. 2009, Hsiung et al. 2018). Thus, we included ENSO events as an additional environmental factor within the model and investigated its degree of influence among the rest of the variables. Finally, a generalized additive model (GAM) was developed to investigate the relationships between biological and environmental factors and variations in *A. japonica* glass eel body length.

2. MATERIALS AND METHODS

2.1. Glass eel collection and total length measurements

The *Anguilla japonica* glass eel surveys were performed in the Yilan River in Yilan County, northeast Taiwan (24.7252° N, 121.8329° E; Fig. 1) during the fishing season (November–March) from 2010 to 2019. Sampling was conducted using fyke nets along the estuary. The captured glass eels were immediately preserved in 95% ethanol after collection (Cheng & Tzeng 1996), and total length (TL) measurements were performed after 1 mo of storage to avoid biases caused by shrinking. In a previous examination of TL shrinkage of *A. japonica* glass eels in our laboratory, we found that the eels shrink by 6% in the first month after capture and then do not change after that (data not shown). In addition, all samples used in this study were collected, stored, and measured using the same procedures. Therefore, TL data should be representative without correction in this study. The individual TL values of specimens were measured to the nearest 0.1 mm, and their pigmentation stages were observed based on techniques established by Tesch & White (2008). The specimens were then classified into either pigment stage 5A or pigment stage 5B (Fig. 1). The former is the earliest phase of the glass eels arriving in estuaries (Tesch & White 2008), and these eels had completed metamorphosis. The specimens at this stage were almost eel-like in form and had no external pigment. On the other hand, at stage 5B, the eels possessed pigmentation in the head and tail region (Fukuda et al. 2013) (Fig. 1). Only glass eels at stage 5A were ultimately used in the present study, as older eels may remain longer in the estuary, and their growth could thus be markedly affected by the estuarine environment. In that case, their growth conditions (TL in the present study) may not reliably reflect the impacts of changes in oceanic environmental conditions.

The entire weekly catch data for *A. japonica* glass eels in Yilan County recorded by the Taiwan Japan-

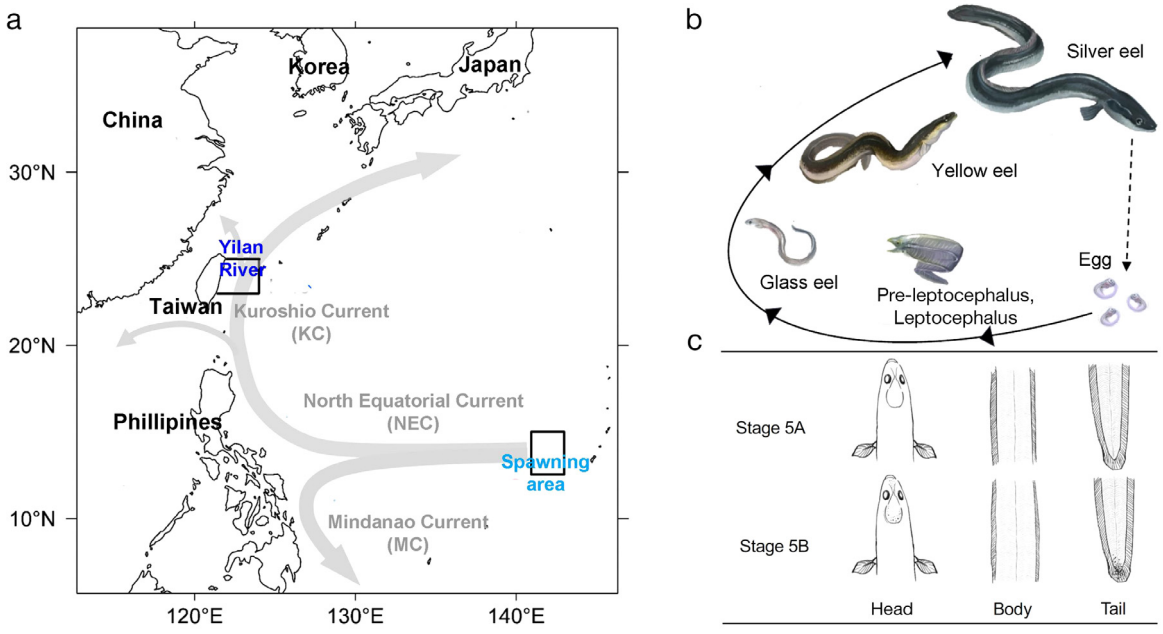

Fig. 1. (a) Schematic view of circulation in the western North Pacific Ocean in regard to *Anguilla japonica* migration. The presumed spawning location of *A. japonica*, including those sampled in the Yilan River and the Kuroshio zone (22–25° N, 121–124° E), was regarded as the effective migration area in the simulation and is indicated on the map. (b) Life history of *A. japonica* and (c) the comparison of pigmentation stages 5A and 5B in *A. japonica* glass eel. Modified from Fukuda et al. (2013)

ese Glass Eel Reporting System (Fisheries Agency, Council of Agriculture, Executive Yuan, Taiwan) from November to March 2010 (hereafter using 2010 to represent data lasting from November 2010 to March 2011) were also collected. The collection of *A. japonica* eggs and newly hatched larvae in the spawning area indicated a synchronized spawning habit of the species during the new moon period (Tsukamoto et al. 2011, Aoyama et al. 2014) that led to the arrival of the recruited glass eels in batches comprising individuals of similar ages (Han et al. 2016). The weekly peaks reflected spawning events of *A. japonica* occurring before the new moon approximately 160–180 d before reaching the offshore area of Yilan. Three spawning events were observed in 2010, 2013, 2015, and 2017 based on data from the Elver Online Reporting System of the Taiwan Fisheries Agency, while 2 events were observed during the other years (Fig. S1 in the Supplement at www.int-res.com/articles/suppl/m683p109_supp.pdf). According to the weekly catch data, the hatching periods were likely to occur primarily in June and July over the study decade (excluding 2017) when spawning extended to September. To confirm that the glass eels within a given group were from the same spawning event, individuals collected during each catch peak week were considered to be the same cohort and were further combined with the TL measurements mentioned above. A total of 2047 glass eels were used to determine TL distribution patterns and possible cohort trends over time.

2.2. Simulation of migration routes

A coupled biological–physical model based on the Lagrangian particle tracking method was used to investigate the potential migration routes of *A. japonica* larvae from the spawning area to the Yilan River that represented the Kuroshio zone in the present study (Fig. 1). Both ocean currents and biological swimming speed were included in the model. The former was extracted from the HYbrid Coordinate Ocean Model (HYCOM) global reanalysis data set (GLBu0.08; https://www.hycom.org/data/glbu0pt08). The HYCOM global reanalysis product applies the Navy Coupled Ocean Data Assimilation (NCODA) system (Cummings 2005, Cummings & Smedstad 2013) for data assimilation. NCODA assimilates available satellite altimeter observations, satellite and *in situ* SST values, and *in situ* vertical temperature and salinity profiles from XBTs, Argo floats, and moored buoys. Surface information is projected downward into the water column using improved synthetic ocean profiles (Helber et al. 2013). The biological swimming speeds increased linearly as age increased,

and an eel larval maximum swimming speed of approximately 3.6 ± 2.7 cm s^{-1} was achieved in a laboratory experiment (Yamada et al. 2009).

We released 2009 particles within a 0.5 × 0.5° grid system per cohort per year from May to September (a total of 18 081 particles) at 12.5–14.9° N and 141–143° E, and this was defined as the eel spawning area in this study. Each particle was considered to be a virtual eel larva in the ocean. The range of the migration routes was established in the areas in proximity to 12.5–25° N and 119–143° E in the simulation and for environmental variable analysis. Based on the new moon hypothesis (Tsukamoto et al. 2003), we estimated the potential hatching day by combining the mean larval period (160 d) that was obtained from the body length data analysis (Han et al. 2016) and the nearest date of the new moon, as the spawning activity on the new moon day appears to be the most obvious day during that period. Thus, only that day was chosen as a representative day. The released particles were tracked for 220 d.

To consider the biological abilities of *A. japonica* in the simulation, the particles were set to drift passively in the first 10 d (simulating stages from preleptocephali to leptocephali; see the eel life cycle in Fig. 1b), allowed to actively swim in the leptocephalus stage from the 11th day to the 150th day, and maintained their metamorphosis to glass eels on the 151st day until the end of the drifting (i.e. arriving at the estuary of the Yilan River) (Chang et al. 2018). As no daily swimming differences of *A. japonica* were observed, consistent swimming patterns and speeds were assumed in this study while accounting for overestimation and/or underestimation. After hatching, the particles exhibited a swimming velocity of 0.01 cm s^{-1} from the 11th day and then increased their swimming velocity by 1.42 cm s^{-1} per month up to a velocity of 6 cm s^{-1}, which represents the maximum observed value of both American and Japanese eel species (Rypina et al. 2014, Chang et al. 2015). Swimming velocity was maintained at 6 cm s^{-1} until the end of the simulation. A similar procedure was applied by Rypina et al. (2014) and Chang et al. (2015) to estimate the migration of American eels from the Sargasso Sea and Japanese eels from their spawning sites in the Western Pacific Ocean, respectively. Moreover, the behavior of *A. japonica* larvae and glass eels (i.e. DVM) was included, as the eel larvae actively swam. The particles were placed at a depth of 50 m at night (18:00–06:00 h) and a depth of 150 m during the day (06:00–18:00 h). The horizontal swimming direction of the larvae was calculated using Eq. (1):

$$u_s1 = V \times \frac{u_c}{\sqrt{u_c^2 + v_c^2}},\ v_s1 = V \times \frac{v_c}{\sqrt{u_c^2 + v_c^2}} \quad (1)$$

Here, u_s1 and v_s1 represent the x and y components of the particle swimming velocity with the current, respectively; V is the eel larval swimming speed, and u_c and v_c are the x and y components of the current velocity, respectively.

Particle locations were recorded every 3 h from the beginning of the simulation. In a cohort case, all potential migration routes are presented in Fig. 2a; however, only particles possessing migration routes into the Kuroshio zone (22–25° N, 121–124° E) were considered effective migration routes (Fig. 2b). This protocol excluded the particles remaining in the western North Pacific Ocean, those entering the MC, and those reaching the Kuroshio before 160 d and after 180 d. Specifically, only particles entering the Kuroshio zone within 160–180 d were used (the expected average ages of the glass eels when they successfully migrated). The final potentially effective migration routes of *A. japonica* resulted in 8 routes in 2010, 36 routes in 2011, 59 routes in 2012, 34 routes in 2013, 99 routes in 2014, 220 routes in 2015, 81 routes in 2016, 95 routes in 2017, and 23 routes in 2018 (Figs. S2 & S3). The environmental data in combination with the successful migration routes and drifting days of each particle in different cohorts for the 9 years are reported in Table S1.

2.3. Environmental data

Three variables, including SST, salinity, and accumulated chl *a* (aChl *a*) concentrations, were included in our subsequent modeling activities to capture the effects of the environment on the TL dynamics of *A. japonica* glass eels. The areas for environmental variable analysis were 12.5–14.9° N, 141–143° E, which was defined as the eel spawning area, and 12.5–25° N, 119–143° E, which was defined as the range of the migration routes in this study. SST and aChl *a* were measured on the surface. The depth for salinity data that were extracted was fixed at 150 m in the spawning area, where the depth was set at 150 m in the morning (06:00–18:00 h) and 50 m at night (18:00–06:00 h) along the migration route. The migration days of each particle (larvae) were different, and this could affect food consumption, with a longer migration time resulting in higher food consumption. *A. japonica* larvae appear to feed on 'marine snow', which is the aggregate of sinking particles, including the remains of jellyfish, larvaceans, salps, and other large zooplankton, clay minerals, phytoplankton, pro-

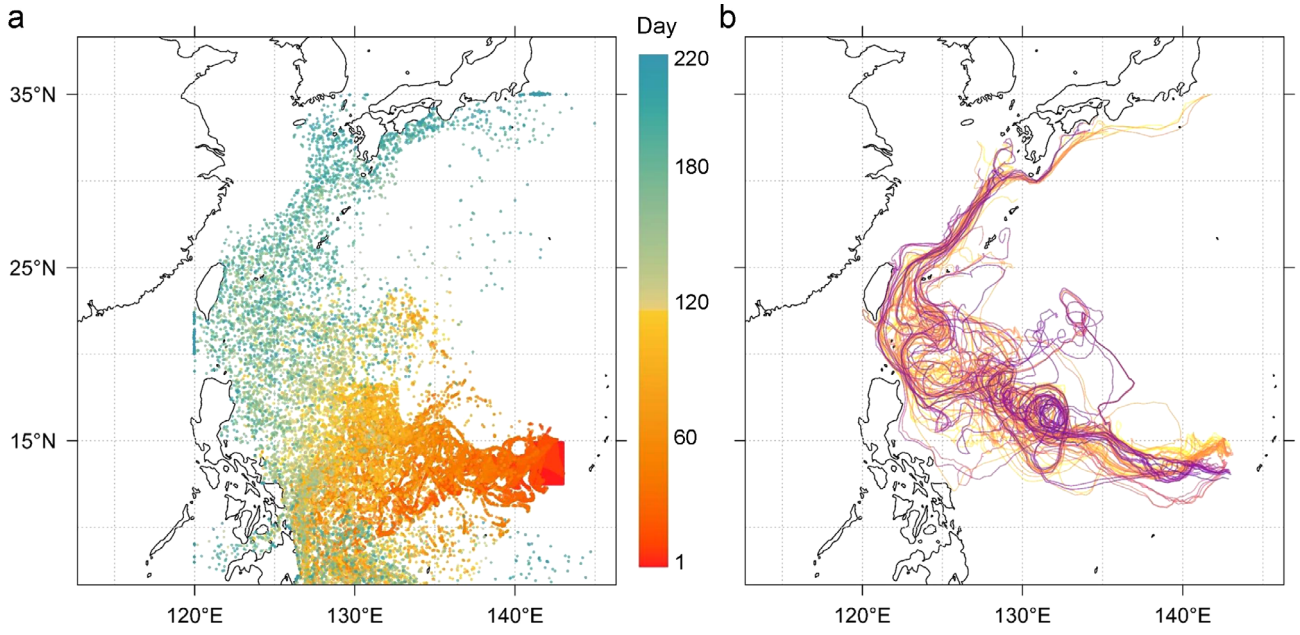

Fig. 2. (a) Distribution of particles (representing *Anguilla japonica* larvae) after release from the spawning area, and (b) effective migration routes using the simulation of the third cohort in 2015 as an example. Color bar in (a) indicates the number of days after the particle release. Lines of different colors in (b) represent individual effective migration routes

tists, and fecal matter (Miller et al. 2013). Marine snow particle production is linked to phytoplankton PP (Alldredge & Jackson 1996, Turner 2002), and chl *a* concentrations are an indicator of phytoplankton abundance and biomass in the ocean. Accordingly, we assumed that aChl *a* and marine snow possess a positive relationship, and we further used aChl *a* concentrations in the analysis of the present study. SST (°C) and salinity (psu) data were obtained from the 1/12° HYCOM output used in the coupled biological–physical model described above. Daily chl *a* (mg m^{-3}) data at a 4 km spatial resolution were obtained from the Copernicus Marine Environment Monitoring Service (http://marine.copernicus.eu/). The Oceanic Niño Index (ONI) was obtained from NOAA (www.cpc.ncep.noaa.gov) to define the 3 ENSO phases of El Niño, La Niña, and normal years.

2.4. Establishing the model

We used a GAM to investigate the effects of environmental variables on the TL dynamics of *A. japonica* glass eels. GAMs enable smooth functions to model the non-linear effect of explanatory variables and can interpret potential connections that are challenging to discern through the use of linear models or simple correlations (Hastie 2017).

The GAM was developed using the TL of *A. japonica* glass eels as the response variable. TL data were simulated by bootstrapping 500 times using 20 distinct cohorts from 2010 to 2019. Therefore, the sample size for the TL estimation was 10 000. The continuous explanatory variables included mean SST, mean salinity (SL), and aChl *a* concentrations in the spawning area and along the migration routes, while the ENSO phase of each year was a nominal explanatory variable. The environmental variables in the spawning area were calculated at the particle release sites during the first 10 d, while those along the migration routes were calculated based on migration days. The formulation of the GAM model in this study is as follows:

$$\text{Length} \sim s(\text{TP.s}) + s(\text{SL.s}) + s(\text{aChl-a.s}) + s(\text{TP.m}) + s(\text{SL.m}) + s(\text{aChl-a.m}) + \text{ENSO Phase} \quad (2)$$

where s extends the domain of the smooth function of the variables. TP.s, SL.s, and aChl-a.s denote the environments of the spawning area, and TP.m, SL.m, and aChl-a.m denote the environment of the migration routes. A Gaussian error distribution combined with an identity link function was applied to the model.

As pre-processing steps in the modeling procedure, colinearity among the covariates was assessed by calculating variance inflation factors (VIF; Zuur et al. 2009). All variables possessing VIF values below a cut-off value of 3 were retained for fitting in the model (Zuur et al. 2010). The model-fitting performance was determined according to the total deviance

explained and Akaike's information criterion (AIC). The best-fitting model was developed using a forward model selection procedure that began from a null model followed by the addition of the most influential variables sequentially and was based on the increased total deviance explained and the AIC of the decrease of the model. When all the variables were included, the model in which the addition of an extra variable did not lead to a substantial increase in model performance was retained as the 'final' model. Diagnostic plots, including a histogram of residuals and a plot of residuals versus linear predictor, were used to evaluate model fitness and statistical assumptions of residuals (normal distribution and homogeneity of variance). All modeling procedures were implemented in R v.3.6.2 (R Development Core Team 2019) using the 'mgcv' package (Wood 2017).

3. RESULTS

3.1. TL and estimated hatching date

From 2010 to 2019, the TL of *Anguilla japonica* glass eels ranged from 48.5 to 65.0 mm, with an average TL of 57.1 mm (Table 1, Fig. 3). TL differed significantly among cohorts and years (Kruskal-Wallis test, all $p < 0.05$). Among cohorts, large differences in TL were observed between the third cohort in 2010 and the second cohort in 2015 (means = 54.7 and 59.2 mm, respectively). The combination of *A. japonica* catch data and TL measurements indicated that the estimated hatching dates were predominantly in June and July, while a small number of larvae hatched in May, August, and September (Table 1).

3.2. Effects of environmental variables on TL

The AIC scores typically decreased with a gradual increase in variables; however, there was little change in the deviance and AIC from the last addition (Table 2). Considering the lowest variables in the model to avoid overfitting and to provide sufficient explanatory power of the model, Model 6 was ultimately selected as the preferred model in this study. The AIC score was 23 850.52, and the total variance explained in the final model was 57.3%. The diagnostic plots of residuals in the final model indicated that the model assumptions (normal distribution and homoscedasticity of the residuals) were not violated (Fig. S4).

Although all selected variables in the final model were highly significant (all $p < 0.001$; Table 3), the environmental variables in the spawning area exerted a greater influence on TL than did those along the migration routes (Table 3). The ENSO phase exerted the greatest impact (67.1%) on the TL values of *A. japonica* glass eels, followed by the mean TP (12%) and aChl *a* concentration (11.4%) in the spawning area. Other variables, including the mean TP (4.5%) and aChl *a* concentration (2.5%) along the migration routes and mean SL in the spawning area (2.5%) also exerted significant effects on TL; however to a much lesser degree.

According to the final model (Fig. 4), when the partial effect (the *y*-axis of the figure) is positive, the parameter exerts an effect on the body length. In contrast, when the partial effect is negative, no effects are observed. The ideal mean TP for obtaining a larger TL for *A. japonica* glass eels ranged from 21–24.5°C (with an optimum mean TP of 22.5°C) in the spawning area. TL values were greater along

Table 1. Mean (±SD) total length (TL; mm), sample size (N), and estimated hatching day of each cohort of juvenile *Anguilla japonica* collected in the Yilan River from 2010 to 2018. NA: no *A. japonica* juveniles were collected in that cohort; see Fig. S1 for weekly catch data. Blank cells: no catch record for the cohort

Year	1st Cohort			2nd Cohort			3rd Cohort		
	TL	N	Estimated hatching date	TL	N	Estimated hatching date	TL	N	Estimated hatching date
2010	NA		14 May	56.3 ± 2.1	168	12 Jun	54.7 ± 2.1	33	12 Jul
2011	57.9 ± 2.2	23	2 Jun	57.6 ± 2.1	71	1 Jul			
2012	56.6 ± 2.2	161	19 Jun	56.7 ± 2.5	60	19 Jul			
2013	57.6 ± 1.8	100	8 Jun	57.5 ± 2.6	102	8 Jul	57.1 ± 2.3	82	7 Aug
2014	56.7 ± 2.9	246	27 Jun	58.7 ± 2.3	89	27 Jul			
2015	58.1 ± 2.0	127	18 May	59.2 ± 2.0	111	16 Jun	58.6 ± 2.2	109	16 Jul
2016	57.6 ± 2.1	109	5 Jun	56.5 ± 2.5	92	4 Jul			
2017	NA		23 Jul	55.6 ± 2.1	109	22 Aug	54.6 ± 2.2	86	20 Sep
2018	56.6 ± 2.3	93	14 Jun	56.1 ± 2.4	76	13 Jul			

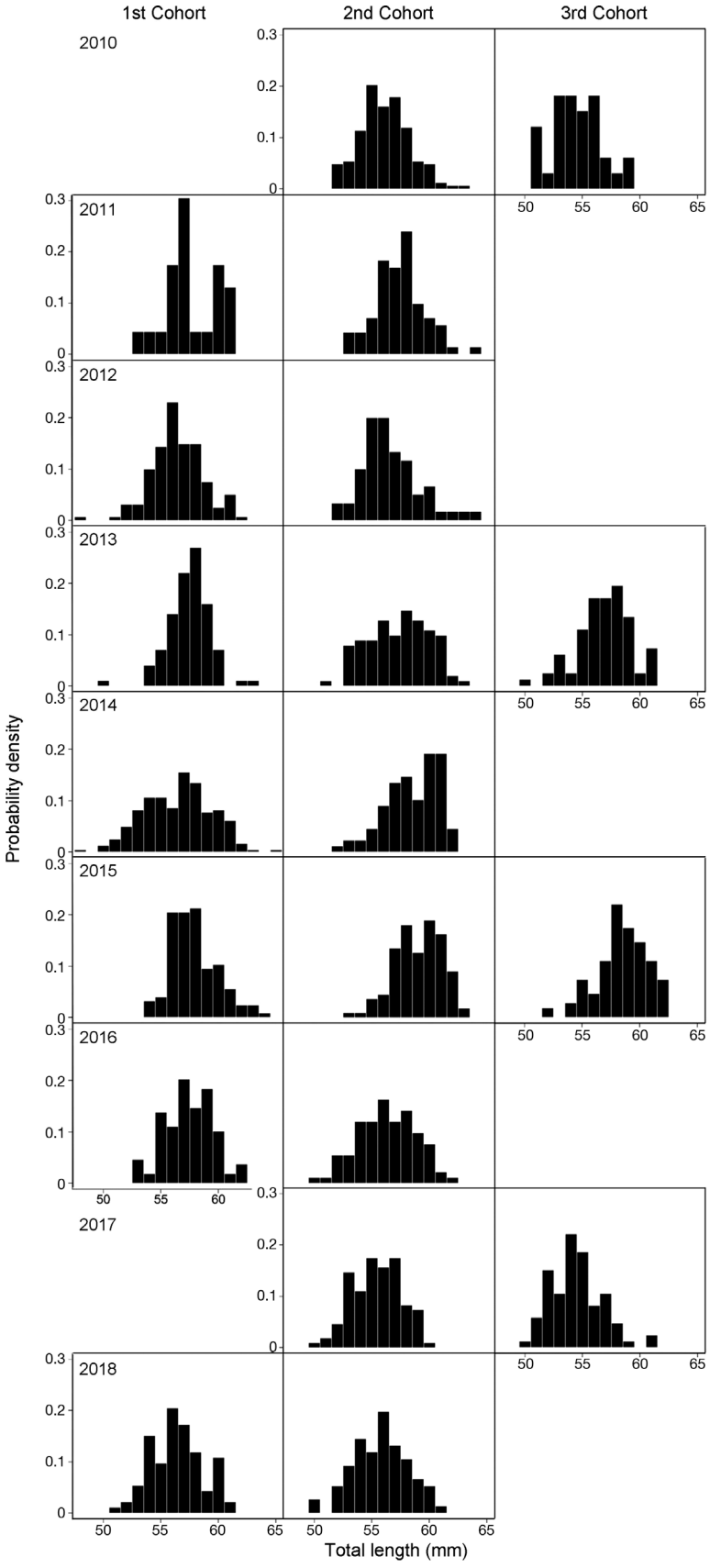

Fig. 3. Probability density distributions of total length based on cohorts of *Anguilla japonica* eels captured in the Yilan River, Taiwan from 2010–2019. A blank represents no catch record for that cohort

the migration routes when the mean TP was higher than 24°C, and the TL exhibited an increasing trend with an increase in mean TP. For the effects of aChl *a* concentration, larger TL values were observed from 0.03 to 0.07 mg m^{-3}, and a negative effect was observed with increasing aChl *a* concentration in the spawning area. Conversely, larger TL values were associated with a higher aChl *a* concentration when this value exceeded 13 mg m^{-3} along the migration routes. The mean SL ranged from 35.1 to 35.3 psu in the spawning area, where the most pronounced peak was approximately 35.25 psu. Regarding ENSO effects, the model revealed that greater TLs were observed during El Niño years compared to those observed during La Niña and normal years.

4. DISCUSSION

Changing oceanic environments in response to contemporary climate change may cause a shift in both the location of the spawning area and the migration routes of *Anguilla japonica*, and this could result in negative effects on their migration during the early life stages (Vecchi et al. 2006, Vecchi & Soden 2007, DiNezio et al. 2009, Collins et al. 2010, Xie et al. 2010, Behrenfeld et al. 2016, Hsiung & Kimura 2019). Therefore, understanding the environmental factors and mechanisms — particularly those that occur during the early life stages of *A. japonica* growth — will not only assist ongoing attempts to propagate this organism artificially but also offer further insights to facilitate eel resource management and conservation under continuous global warming conditions. We explored these hypotheses by examining the potential ef-

Table 2. Generalized additive model selection process that includes El Niño–Southern Oscillation (ENSO) phase, sea surface temperature of the spawning area (TP.s), accumulated chl *a* concentration of the spawning area (aChl-a.s), salinity of the spawning area (SL.s), sea surface temperature on the migration routes (TP.m), accumulated chl *a* concentration on the migration routes (aChl-a.m), and salinity on the migration routes (SL.m) as explanatory variables for *Anguilla japonica* juvenile total length. Models were selected using Akaike's information criteria (AIC). Model 6 (in **bold**) was ultimately selected as the preferred model for the eel total length data. ΔAIC indicates the step-wise reduction in AIC as variables are added to the first model

Model	Deviance explained (%)	AIC	ΔAIC
Null		32376.66	8526.1
Mod1: ENSO phase	38.5	27431.94	3581.4
Mod2: Mod1+TP.s	45.4	26253.62	2403.1
Mod3: Mod2+aChl-a.s	51.9	24987.91	1137.4
Mod4: Mod3+TP.m	54.5	24469.10	618.6
Mod5: Mod4+ aChl-a.m	55.9	24167.89	317.8
Mod6: Mod5+SL.s	**57.3**	**23850.52**	**0**
Mod7: Mod6+SL.m	57.9	23731.77	−118.8

Table 3. Individual contributions of selected environmental variables within the final generalized additive model, including El Niño–Southern Oscillation (ENSO) phase, sea surface temperature of the spawning area (TP.s), accumulated chl *a* concentration of the spawning area (aChl-a.s), sea surface temperature on the migration routes (TP.m), accumulated chl *a* concentration on the migration routes (aChl-a.m), and salinity of the spawning area (SL.s). edf: estimated degree of freedom; p-value indicates probability; total deviance explained denotes the percentage of model total deviance explained by each variable

Variable	edf	p	Deviance explained (%)
ENSO phase	2	<0.001	67.1
TP.s	6.668	<0.001	12
aChl-a.s	5.539	<0.001	11.4
TP.m	8.771	<0.001	4.5
aChl-a.m	8.629	<0.001	2.5
SL.s	8.63	<0.001	2.5

fects of several environmental factors, including SST, salinity, and chl *a* concentration, on the growth of *A. japonica* during the larval and glass eel stages by combining particle tracking and oceanic environmental data with long-term TL analyses of *A. japonica* glass eels. The flexibility of the GAM facilitated assessment of the interactions between the TL of *A. japonica* glass eels and environmental factors.

Our results indicate that environmental conditions present in the spawning area may exert a larger influence on Japanese eel growth than along the migration route (Table 3). This might occur because the larvae in the spawning area are the most sensitive to environmental changes, while larger larvae on migration routes may exhibit a better survival potential in regards to tolerating a wider range of environmental changes (Houde 1989, Anderson 1998). Conversely, for the European eel *A. anguilla* and American eels *A. rostrata*, Hanel et al. (2014) reported that it is difficult to disentangle the underlying reason for a decrease in larval abundance or lower eventual recruitment; however, it may be due to lower survival of early life stages in the Sargasso Sea or to a reduction of spawners that arrive at the spawning ground (Miller et al. 2016). The unfavorable conditions within the spawning area in the Sargasso Sea might be a possible reason for the decrease.

In addition to the effects of environmental factors along the migration routes and in the spawning area, the present study demonstrated that TL was significantly larger during the El Niño years and lower during La Niña years (Fig. 4). Body length has been reported to be strongly correlated with daily age based on otolith measurements (Tsukamoto et al. 1992, Ishikawa et al. 2001). Previous studies have also demonstrated that larval duration is significantly longer during El Niño years due to shifts in the NEC bifurcation and salinity front, and this may lead to larvae encountering slower currents in addition to extending the separation between the spawning area and the NEC bifurcation (Hsiung et al. 2018). Therefore, ENSO events may exert the most significant influence on the growth of Japanese eels in the early life stages, while the aChl *a* concentrations along the migration routes could be another important factor that simultaneously affects larval growth.

*A. japonic*a larvae appear to begin to perform DVM after reaching a certain size, as individuals of 10–20 mm TLs have been caught at 50–100 m depths with temperatures of 26–29°C at night and at 130–250 m depths with temperatures of 17–26°C during the daytime (Otake et al. 1998). This behavior indicates that *A. japonica* larvae (>10 mm TL) can adapt to a wide range of temperatures. However, some studies have demonstrated that *A. japonica* leptocephali exhibit superior growth performance (as compared to lower temperatures) when reared at 24–25°C in a laboratory (Okamura et al. 2018), and this is consistent with our findings that TL was greater when the sea temperature along the migration route was higher than 24°C in the simulation. Additionally, the duration of the larval stage of cultured *A. japonica* glass eels can be shortened to that observed in the glass eels collected from the wild when they are reared in captivity at 25–27°C

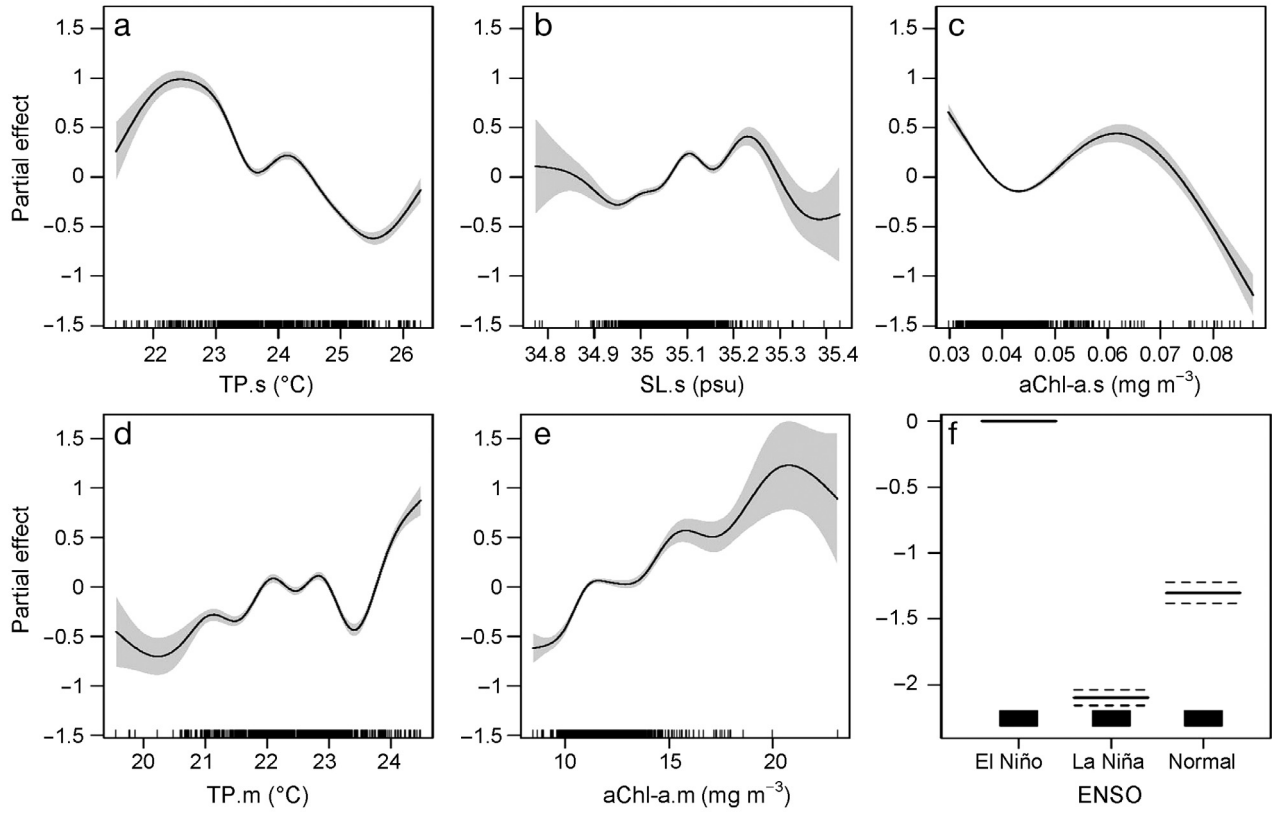

Fig. 4. Partial effects generated by the final generalized additive model (GAM) selected in this study and the relationships between the total length of *Anguilla japonica* glass eels and (a) mean sea surface temperature of the spawning area (TP.s), (b) salinity of the spawning area (SL.s), (c) accumulated chl *a* concentration of the spawning area (aChl-a.s), (d) mean sea surface temperature on the migration routes (TP.m), (e) accumulated chl *a* concentration on the migration routes (aChl-a.m), and (f) El Niño–Southern Oscillation (ENSO) phase on *A. japonica* juvenile total length from the GAM in the final model. The *y*-axis is the partial effect of the variable; shaded section shows the 95% SE confidence intervals. The relative density of data points is presented on the 'rug' on the *x*-axis. The dotted line in (f) represents 95% SE confidence intervals

(Masuda et al. 2011). In contrast, Kurokawa et al. (2008) and Ahn et al. (2012) demonstrated that the rate of occurrence of morphological deformities in cultured glass eels was lower at 24–28°C than it was at 20–22°C, and egg hatching was more efficient at 25°C than it was at lower temperatures. Furthermore, a recent study reported that the temperature that *A. japonica* larvae experienced in the spawning area (~150 m) was approximately 26.3 ± 0.8 to 26.7 ± 0.4°C, according to analyses of the oxygen isotope ratios of the core region of the otoliths of *A. japonica* glass eels, and this temperature corresponds to the uppermost part of the thermocline and chlorophyll maximum in the vertical hydrographic profile (Shirai et al. 2018).

A. japonica larvae feed on marine snow particles that consist of a variety of organic matter types (Miller et al. 2013). Marine snow particle production is linked to phytoplankton PP (Alldredge & Jackson 1996, Turner 2002). In the present study, the aChl *a* concentration was used as an indicator of PP or as the food source of Japanese eel larvae, and as expected, a positive correlation was observed between larval TL and aChl *a* concentration along the migration routes. The aChl *a* concentration in the spawning area may be greater than the threshold required for feeding and survival.

Miller et al. (2016) proposed that density-dependent larval survival could occur in 3 Northern Hemisphere eel species (including the Japanese eel) due to their synchronized spawning behavior, whereby all female anguillid eels spawn millions of eggs simultaneously in the spawning area. Thus, all larvae would hatch in the same location. Miller et al. (2019) further reported that *A. anguilla* spawned across a 2000 km wide region of the North Atlantic Ocean. However, adult eels begin their spawning migrations out of freshwater during many months of each year, and based on this, it is uncertain if all eels can reach all parts of the spawning area during the main spawning season. Eels that migrate early or from areas closer to the North At-

lantic and possess adequate time and energy may swim to the western side of the spawning area, while those that migrate later and from farther away or that possess low energy reserves could spawn in the east. Therefore, it is possible that the larvae spawned by the same or similar cohort of adult eels may hatch on one or the other side. Additionally, there are approximately 4–7 anguillid and mesopelagic eel species spawning sympatrically with the Japanese eel (Yoshinaga et al. 2011). Consequently, larvae from one or several species can simultaneously compete for marine snow particles. Based on the density-dependent effect, larval abundance in the spawning area could influence the food resources exploited by each larva. Therefore, assessing the relationship between aChl *a* concentration in the spawning area and the growth of *A. japonica* larvae would be challenging without considering larval abundance.

Although salinity influences the locations of the *A. japonica* spawning sites (Kimura et al. 1994, Kimura & Tsukamoto 2006), unlike TP and aChl *a* concentration, it did not exert significant effects on growth conditions during the early life stages in the present study. This result is consistent with the findings of previous studies demonstrating that older *A. japonica* larvae can tolerate a broad range of salinity conditions (Chang 2004, Okamura et al. 2009); however, early-stage larvae are more likely to develop morphological deformities at salinities lower than 33 psu or higher than 42 psu (Okamoto et al. 2009). Conversely, it may be difficult to determine strong correlations with the average values over such a large analysis region.

The influence of ENSO events on *A. japonica* transport during early life stages has been evaluated in several studies (Kimura et al. 2001, Kim et al. 2007, Zenimoto et al. 2009, Hsiung et al. 2018). In addition to the effects of environmental conditions along the migration routes and in the spawning area, the findings of the present study indicated that the TL values of glass eels (stage 5A) were greater during El Niño versus La Niña years when arriving at the estuaries in northern Taiwan. As previous studies have demonstrated that body length is highly correlated with daily age (Tsukamoto et al. 1992, Ishikawa et al. 2001), we assumed that the larval duration of *A. japonica* glass eels should be longer during El Niño years and lower during La Niña years. Our results also support those of a previous study that observed a longer *A. japonica* larval duration during El Niño years than that observed during La Niña years due to the shifting of the NEC bifurcation and NEC salinity front (Hsiung et al. 2018). Such shifts could cause the larvae to encounter slower currents that would extend the journey time between the spawning area and the NEC bifurcation (Hsiung et al. 2018).

5. CONCLUSIONS

This study revealed that the biological changes in oceanic environmental conditions such as chl *a* concentrations, salinity, and temperature may play key roles in eel migration and may influence mortality, growth conditions, food availability, and the migration process, thus further affecting the growth of the glass eels prior to their arrival at the estuary. Conversely, ENSO events primarily affect the duration of growth of the glass eels before they arrive at the estuary by causing physical changes in the spawning area and migration route. In addition to revealing the most significant factors, the results of our study may assist in ongoing attempts to propagate the study species artificially. Global warming can significantly alter oceanic environments, particularly current velocity distribution, salinity, and plankton growth and distribution (Vecchi et al. 2006, Vecchi & Soden 2007, DiNezio et al. 2009, Collins et al. 2010, Xie et al. 2010, Behrenfeld et al. 2016), and it can significantly influence the transport process and distribution of *Anguilla japonica* (Hsiung & Kimura 2019). Therefore, the findings of this study will facilitate further research examining the potential impacts of global warming on the physical and biological characteristics of the Japanese eel.

Acknowledgements. The authors thank the Ministry of Science and Technology, Executive Yuan, Taiwan (MOST 106-2313-B-002-036-MY3; MOST 109-2313-B-002-001-MY2), the Council of Agriculture, Executive Yuan, Taiwan (106AS-11.3.4-FA-F1; 110-FRM-2.17-G-03), and the State Key Laboratory of Ocean Engineering, Shanghai Jiao Tong University, PR China (GKZD010075) for funding this project.

LITERATURE CITED

Ahn H, Yamada Y, Okamura A, Horie N, Mikawa N, Tanaka S, Tsukamoto K (2012) Effect of water temperature on embryonic development and hatching time of the Japanese eel *Anguilla japonica*. Aquaculture 330-333:100–105

Alldredge AL, Jackson GA (1996) Aggregation in marine systems. Deep Sea Res II 42:1–7

Anderson CS (1998) Partitioning total size selectivity of gill nets for walleye (*Stizostedion vitreum*) into encounter, contact, and retention components. Can J Fish Aquat Sci 55:1854–1863

Aoki K, Yamamoto T, Fukuda N, Yokouchi K and others (2018) Enhanced local recruitment of glass eel *Anguilla japonica* in Oyodo River, Miyazaki and offshore environmental conditions in 2002. Fish Sci 84:777–785

Aoyama J, Watanabe S, Miller MJ, Mochioka N, Otake T, Yoshinaga T, Tsukamoto K (2014) Spawning sites of the Japanese eel in relation to oceanographic structure and the West Mariana Ridge. PLOS ONE 9:e88759

Behrenfeld MJ, O'Malley RT, Boss ES, Westberry TK and others (2016) Revaluating ocean warming impacts on global phytoplankton. Nat Clim Chang 6:323–330

Blaxter JHS (1991) The effect of temperature on larval fishes. Neth J Zool 42:336–357

Bonhommeau S, Chassot E, Rivot E (2008) Fluctuations in European eel (*Anguilla anguilla*) recruitment resulting from environmental changes in the Sargasso Sea. Fish Oceanogr 17:32–44

Chang YC (2004) Studies on the salinity tolerance of larvae of Japanese eel (*Anguilla japonica*). J Taiwan Fish Res 12:25–31

Chang YL, Sheng J, Ohashi K, Béguer Pon M, Miyazawa Y (2015) Impacts of interannual ocean circulation variability on Japanese eel larval migration in the western North Pacific Ocean. PLOS ONE 10:e0144423

Chang YLK, Miyazawa Y, Miller MJ, Tsukamoto K (2018) Potential impact of ocean circulation on the declining Japanese eel catches. Sci Rep 8:5496

Cheng PW, Tzeng WN (1996) Timing of metamorphosis and estuarine arrival across the dispersal range of the Japanese eel *Anguilla japonica*. Mar Ecol Prog Ser 131: 87–96

Collins M, An SI, Cai W, Ganachaud A and others (2010) The impact of global warming on the tropical Pacific Ocean and El Niño. Nat Geosci 3:391–397

Cummings JA (2005) Operational multivariate ocean data assimilation. Q J R Meteorol Soc 131:3583–3604

Cummings JA, Smedstad OM (2013) Variational data assimilation for the global ocean. In: Xu L, Park SK (eds) Data assimilation for atmospheric, oceanic and hydrologic applications, Vol 2. Springer, Cham, p 303–343

Dekker W (2004) Slipping through our hands: population dynamics of the European eel. PhD thesis, Universiteit van Amsterdam

DiNezio PN, Clement AC, Vecchi GA, Soden BJ, Kirtman BP, Lee SK (2009) Climate response of the equatorial Pacific to global warming. J Clim 22:4873–4892

Elie P, Rochard E (1994) Migration des civelles d'anguilles (*Anguilla anguilla* L.) dans les estuaires, modalités du phénomène et caractéristiques des individus. Bull Fr Pêche Piscic 335:81–98

Fukuda N, Miller MJ, Aoyama J, Shinoda A, Tsukamoto K (2013) Evaluation of the pigmentation stages and body proportions from the glass eel to yellow eel in *Anguilla japonica*. Fish Sci 79:425–438

Gascuel D (1986) Flow-carried and active swimming migration of the glass eel (*Anguilla anguilla*) in the tidal area of a small estuary on the French Atlantic coast. Helgol Meeresunters 40:321–326

Han YS, Zhang H, Tseng YH, Shen ML (2012) Larval Japanese eel (*Anguilla japonica*) as sub-surface current bio tracers on the East Asia continental shelf. Fish Oceanogr 21:281–290

Han YS, Wu CR, Iizuka Y (2016) Batch-like arrival waves of glass eels of *Anguilla japonica* in offshore waters of Taiwan. Zool Stud 55:e36

Han YS, Hsiung KM, Zhang H, Chow LY and others (2019) Dispersal characteristics and pathways of Japanese glass eel in the East Asian continental shelf. Sustainability 11: 2572

Hanel R, Stepputtis D, Bonhommeau S, Castonguay M and others (2014) Low larval abundance in the Sargasso Sea: new evidence about reduced recruitment of the Atlantic eels. Naturwissenschaften 101:1041–1054

Hastie TJ (2017) Generalized additive models. In: Chambers JM, Hastie TJ (eds) Statistical models in S. CRC Press, Boca Raton, FL, p 249–307

Helber RW, Townsend TL, Barron CN, Dastugue JM, Carnes MR (2013) Validation test report for the Improved Synthetic Ocean Profile (ISOP) system, Part I: synthetic profile methods and algorithm. Naval Research Lab, Stennis Detachment, Stennis Space Center, MS

Houde ED (1989) Subtleties and episodes in the early life of fishes. J Fish Biol 35:29–38

Houde ED (2008) Emerging from Hjort's shadow. J Northwest Atl Fish Sci 41:53–70

Hsiung K, Kimura S (2019) Impacts of global warming on larval and juvenile transport of Japanese eels (*Anguilla japonica*). Deep Sea Res II 169–170:104685

Hsiung KM, Kimura S, Han YS, Takeshige A, Iizuka Y (2018) Effect of ENSO events on larval and juvenile duration and transport of Japanese eel (*Anguilla japonica*). PLOS ONE 13:e0195544

Hsu AC, Xue H, Chai F, Xiu P, Han YS (2017) Variability of the Pacific North Equatorial Current and its implications on Japanese eel (*Anguilla japonica*) larval migration. Fish Oceanogr 26:251–267

Ishikawa S, Suzuki K, Inagaki T, Watanabe S and others (2001) Spawning time and place of the Japanese eel *Anguilla japonica* in the North Equatorial Current of the western North Pacific Ocean. Fish Sci 67:1097–1103

Jacoby D, Gollock M (2014) *Anguilla anguilla*. The IUCN Red List of Threatened Species 2014:eT60344A45833138

Kajihara T (1988) Distribution of *Anguilla japonica* leptocephali in western Pacific during September 1986. Bull Jpn Soc Sci Fish 54:929–933

Kim H, Kimura S, Shinoda A, Kitagawa T, Sasai Y, Sasaki H (2007) Effect of El Niño on migration and larval transport of the Japanese eel (*Anguilla japonica*). ICES J Mar Sci 64:1387–1395

Kimura S, Tsukamoto K (2006) The salinity front in the North Equatorial Current: a landmark for the spawning migration of the Japanese eel (*Anguilla japonica*) related to the stock recruitment. Deep Sea Res II 53:315–325

Kimura S, Tsukamoto K, Sugimoto T (1994) A model for the larval migration of the Japanese eel: roles of the trade winds and salinity front. Mar Biol 119:185–190

Kimura S, Inoue T, Sugimoto T (2001) Fluctuation in the distribution of low salinity water in the North Equatorial Current and its effect on the larval transport of the Japanese eel. Fish Oceanogr 10:51–60

Kurokawa T, Okamoto T, Gen K, Uji S and others (2008) Influence of water temperature on morphological deformities in cultured larvae of Japanese eel, *Anguilla japonica*, at completion of yolk resorption. J World Aquacult Soc 39:726–735

Liao IC (2001) A general review on aquaculture in Asia: a focus on Anguilla eel. In: Liao IC (ed) Keynote addresses, 5th and 6th Asian fish forums. AFS Special Publication No. 11. Asian Fisheries Society, Taiwan, p 39–54

Masuda Y, Imaizumi H, Oda K, Hashimoto H, Teruya K, Usuki H (2011) Japanese eel *Anguilla japonica* larvae can metamorphose into glass eel within 131 days after hatching in captivity. Bull Jpn Soc Sci Fish 77:416–418 (in Japanese)

Miller MJ, Chikaraishi Y, Ogawa NO, Yamada Y, Tsukamoto K, Ohkouchi N (2013) A low trophic position of Japanese eel larvae indicates feeding on marine snow. Biol Lett 9:20120826

Miller MJ, Feunteun E, Tsukamoto K (2016) Did a 'perfect storm' of oceanic changes and continental anthropogenic impacts cause northern hemisphere anguillid recruitment reductions? ICES J Mar Sci 73:43–56

Miller MJ, Westerberg H, Sparholt H, Wysujack K and others (2019) Spawning by the European eel across 2000 km of the Sargasso Sea. Biol Lett 15:20180835

Nitani H (1972) Beginning of the Kuroshio. In: Stommel H, Yashida K (eds) Kuroshio: physical aspects of the Japan current. University of Washington Press, Seattle, WA, p 129–163

Okamoto T, Kurokawa T, Gen K, Murashita K and others (2009) Influence of salinity on morphological deformities in cultured larvae of Japanese eel, *Anguilla japonica*, at completion of yolk resorption. Aquaculture 293:113–118

Okamura A, Yamada Y, Mikawa N, Horie N and others (2009) Growth and survival of eel leptocephali (*Anguilla japonica*) in low-salinity water. Aquaculture 296:367–372

Okamura A, Horie N, Mikawa N, Yamada Y, Tsukamoto K (2018) Influence of temperature and feeding regimes on growth and notochord deformity in reared *Anguilla japonica* leptocephali. Fish Sci 84:505–512

Otake T, Inagaki T, Hasumoto H, Mochioka N, Tsukamoto K (1998) Diel vertical distribution of *Anguilla japonica* leptocephali. Ichthyol Res 45:208–211

R Development Core Team (2019) R: a language and environment for statistical computing. R Foundation for Statistical Computing, Vienna

Rilling GC, Houde ED (1999) Regional and temporal variability in distribution and abundance of bay anchovy (*Anchoa mitchilli*) eggs, larvae, and adult biomass in the Chesapeake Bay. Estuaries 22:1096

Rypina II, Llopiz JK, Pratt LJ, Lozier MS (2014) Dispersal pathways of American eel larvae from the Sargasso Sea. Limnol Oceanogr 59:1704–1714

Shinoda A, Aoyama J, Miller MJ, Otake T and others (2011) Evaluation of the larval distribution and migration of the Japanese eel in the western North Pacific. Rev Fish Biol Fish 21:591–611

Shirai K, Otake T, Amano Y, Kuroki M and others (2018) Temperature and depth distribution of Japanese eel eggs estimated using otolith oxygen stable isotopes. Geochim Cosmochim Acta 236:373–383

Tabeta O, Takai T (1975) Leptocephalus of *Anguilla japonica* found in the waters south of Taiwan. Jpn J Ichthyol 22:100–103

Takeuchi A, Higuchi T, Watanabe S, Miller MJ and others (2021) Several possible spawning sites of the Japanese eel determined from collections of their eggs and preleptocephali. Fish Sci 87:339–352

Tanaka H (2003) Techniques for larval rearing. In: Aida K, Tsukamoto K, Yamauchi K (eds) Eel biology. Springer, Berlin, p 427–434

Tesch FW, White RJ (2008) The eel. John Wiley & Sons, New York, NY

Toole JM, Millard RC, Wang Z, Pu S (1990) Observations of the Pacific North Equatorial Current bifurcation at the Philippine coast. J Phys Oceanogr 20:307–318

Tosi L, Spampanato A, Sola C, Tongiorgi P (1990) Relation of water odour, salinity and temperature to ascent of glass eels, *Anguilla anguilla* (L.): a laboratory study. J Fish Biol 36:327–340

Tsukamoto K (1992) Discovery of the spawning area for Japanese eel. Nature 356:789–791

Tsukamoto K (2006) Oceanic biology: spawning of eels near a seamount. Nature 439:929

Tsukamoto K (2009) Oceanic migration and spawning of anguillid eels. J Fish Biol 74:1833–1852

Tsukamoto K, Umezawa A, Ozawa T (1992) Age and growth of *Anguilla japonica* leptocephali collected in Western North Pacific in July 1990. Bull Jpn Soc Sci Fish 58: 457–459

Tsukamoto K, Otake T, Mochioka N, Lee TW and others (2003) Seamounts, new moon and eel spawning: the search for the spawning site of the Japanese eel. Environ Biol Fishes 66:221–229

Tsukamoto K, Chow S, Otake T, Kurogi H and others (2011) Oceanic spawning ecology of freshwater eels in the western North Pacific. Nat Commun 2:179

Turner JT (2002) Zooplankton fecal pellets, marine snow and sinking phytoplankton blooms. Aquat Microb Ecol 27:57–102

Tzeng WN (2003) The processes of onshore migration of the Japanese eel *Anguilla japonica* as revealed by otolith microstructure. In: Aida K, Tsukamoto K, Yamauchi K (eds) Eel biology. Springer, Berlin, p 181–190

Vecchi GA, Soden BJ (2007) Global warming and the weakening of the tropical circulation. J Clim 20:4316–4340

Vecchi GA, Soden BJ, Wittenberg AT, Held IM, Leetmaa A, Harrison MJ (2006) Weakening of tropical Pacific atmospheric circulation due to anthropogenic forcing. Nature 441:73–76

Wood SN (2017) Generalized additive models: an introduction with R. CRC Press, Boca Raton, FL

Xie SP, Deser C, Vecchi GA, Ma J, Teng H, Wittenberg AT (2010) Global warming pattern formation: sea surface temperature and rainfall. J Clim 23:966–986

Yamada Y, Okamura A, Mikawa N, Utoh T and others (2009) Ontogenetic changes in phototactic behavior during metamorphosis of artificially reared Japanese eel *Anguilla japonica* larvae. Mar Ecol Prog Ser 379:241–251

Yoshinaga T, Miller MJ, Yokouchi K, Otake T and others (2011) Genetic identification and morphology of naturally spawned eggs of the Japanese eel *Anguilla japonica* collected in the western North Pacific. Fish Sci 77: 983–992

Zenimoto K, Kitagawa T, Miyazaki S, Sasai Y, Sasaki H, Kimura S (2009) The effects of seasonal and interannual variability of oceanic structure in the western Pacific North Equatorial Current on larval transport of the Japanese eel *Anguilla japonica.* J Fish Biol 74: 1878–1890

Zenitani H, Kono N, Tsukamoto Y (2007) Relationship between daily survival rates of larval Japanese anchovy (*Engraulis japonicus*) and concentrations of copepod nauplii in the Seto Inland Sea, Japan. Fish Oceanogr 16: 473–478

Zhang L, Wang FJ, Wang Q, Hu S, Wang F, Hu D (2017) Structure and variability of the North Equatorial Current/Undercurrent from mooring measurements at 130°E in the Western Pacific. Sci Rep 7:46310

Zuur A, Ieno EN, Walker N, Saveliev AA, Smith GM (2009) Mixed effects models and extensions in ecology with R. Springer Science & Business Media, New York, NY

Zuur AF, Ieno EN, Elphick CS (2010) A protocol for data exploration to avoid common statistical problems. Methods Ecol Evol 1:3–14

Editorial responsibility: Myron Peck, Den Burg, The Netherlands
Reviewed by: M. Kuroki and 2 anonymous referees

Submitted: December 8, 2020
Accepted: October 13, 2021
Proofs received from author(s): January 28, 2022